J Paleolimnol (2008) 40:987–1002
DOI 10.1007/s10933-008-9211-9

ORIGINAL PAPER

A 1,100-year palaeoenvironmental record inferred from stable isotope and trace element compositions of ostracode and plant caryopses in sediments of Cattle Pond, Dongdao Island, South China Sea

Xiaodong Liu · Liguang Sun · Gangjian Wei · Yuhong Wang · Hong Yan · Kexin Liu · Xiaohong Wu

Received: 31 October 2007 / Accepted: 1 April 2008 / Published online: 29 May 2008

Abstract Abundant ostracode valves (*Cyprinotus cingalensis*) and caryopses of *Urochloa paspaloides*, a terrestrial grass, were well preserved in the lacustrine sediments of the Cattle Pond on Dongdao Island, South China Sea. Oxygen and carbon isotopes, and elements (Ca, Mg) were analyzed on ostracode valves and plant caryopses in this study. The $\delta^{18}O_{ostracode}$ and $\delta^{13}C_{ostracode}$ exhibited a positive and statistically significant correlation, and showed a decreasing trend toward the top of sediment sequence with some fluctuations, indicating a gradual increase in effective moisture. The Mg/Ca ratios in the ostracode shells, generally used as a proxy for salinity changes in lake water, showed a trend toward lower values in the upper samples, reflecting a gradual decrease of salinity in the lake. The $\delta^{13}C_{org}$ values in the plant caryopses of the upper 14 cm of sediment have lower values than those in the bottom sediments, suggesting less water and salinity stress. These results indicate increasing effective moisture and rainfall intensity over the past ~1,100 years on Dongdao Island.

Keywords Stable isotopes · Mg/Ca ratios · Historical precipitation · Tropical cyclone frequency · Ostracodes · Caryopses · Lacustrine sediments · Dongdao Island of South China Sea

X. Liu (✉) · L. Sun (✉) · H. Yan
Institute of Polar Environment, University of Science and Technology of China, Hefei, Anhui 230026, China
e-mail: ycx@ustc.edu.cn

L. Sun
e-mail: slg@ustc.edu.cn

G. Wei
Guangzhou Institute of Geochemistry, Chinese Academy of Sciences, Guangzhou 510640, China

Y. Wang
National Institutes of Health, Bethesda, MD 20892, USA

K. Liu
Key Laboratory of Heavy Ion Physics, MOE & Institute of Heavy Ion Physics, Peking University, Beijing 100871, China

X. Wu
School of Archaeology and Museology, Peking University, Beijing 100871, China

Introduction

Tropical cyclones are an important component of the ocean-atmosphere climate system. They account for a significant fraction of damage, injury and loss of life from natural hazards, and their research is gaining increased attention (Chan and Shi 1996; Emanuel 2005; Hoyos et al. 2006). Recent studies suggested that the increase in hurricane frequency and intensity in recent decades might be linked to rising tropical sea surface temperature (SST) and thus global warming (Webster et al. 2005; Hoyos et al. 2006).

The frequency and intensity of tropical cyclones are likely controlled by both natural and anthropogenic factors. Objective estimation of the effect of recent global warming on tropical cyclones requires a good understanding of their natural variability. Unfortunately, observational records of tropical cyclone activities are generally restricted to recent decades because long-term and continuous data are difficult to obtain. On such a short time scale, it is difficult to identify the variability of tropical cyclone frequency and separate anthropogenic signals from natural, multidecadal oscillations (Landsea 2005). To obtain longer records of tropical cyclones, proxy records must be used. However, research on the frequency and intensity of prehistoric tropical storms or cyclones is usually based on lithologic analysis of sediments and coral blocks (e.g. Liu and Fearn 2000; Donnelly et al. 2001; Nott 2004; Yu et al. 2004). More recently, some researchers have used grain size and organic geochemical proxies to reconstruct catastrophic hurricane history (Donnelly and Woodruff 2007; Lambert et al. 2008).

Tropical cyclones in the northwestern Pacific have the highest frequency and intensity worldwide, and the South China Sea is one of the three main centers of tropical cyclones. The Xisha Islands (15°47′–17°08′ N, 111°10′–112°55′ E), in the center of the South China Sea, are under the influence of the East-Asia monsoon. The dry and wet seasons are very distinct due to the monsoon effect (Liu et al. 2006). From June to November, the Xisha Islands are subject to the effect of the southwest monsoons, very frequent tropical cyclones, and heavy precipitation; about 87% of total precipitation (about 1,500 mm) occurs in these months. From December to May is the dry season due to the influence of northeast monsoons, and the precipitation amount is generally less than 15% of the annual total. Meteorological data show that the frequent occurrence of tropical cyclones is generally associated with intense convergence convection, and has a significant contribution to the total precipitation of this area.

Paleoenvironmental and paleoclimatological reconstructions can be accomplished using several analytical approaches. In general, ostracode shell calcification takes place very quickly, from a few hours to several days, in geochemical equilibrium with the water in which it is formed, and composition of the valves does not change once they are formed (Ortiz et al. 2006). Thus, the isotope (and trace element) composition of ostracode shells records chemical conditions of the lake water (e.g. temperature, salinity, dissolved ion composition, hydrology), and can be used as proxies for environmental changes (Schwalb et al. 1995, 1999, 2002; Schwalb and Dean 1998, 2002; Schwalb 2003; Leng and Marshall 2004; Dettman et al. 2005; Anadón et al. 2006; Bahr et al. 2006). In our previous study, we performed detailed sedimentological and elemental geochemical analyses on a sediment core from a small fresh lake on Dongdao Island, South China Sea, and reconstructed the historical record of seabird populations on this Island between 1,350 and 350 yr BP (Liu et al. 2006). In this paper, we analyze carbon and oxygen isotopes and Mg/Ca ratios of ostracodes, as well as organic carbon isotopes of the monospecific caryopsis remains of *Urochloa paspaloides* in the lacustrine sediments. We used these data to reconstruct a ~1,100-year record of precipitation that may reflect a historical trend in tropical cyclones in the Xisha area.

Study area

Dongdao Island (16°39′–16°41′ N, 112°43′–112°45′ E) is one of the eastern islands of the Xisha Island group, South China Sea. It is an elliptical, tropical reef island with a northwest-southeast orientation (Fig. 1). Dongdao Island developed on an individual reef flat, and was formed during the mid to late Holocene, the primary formation period of the Xisha Islands. It has a land area of 1.55 km^2 and an elevation of about 3–6 m, a maximum south-north extension of ~2.0 km, and a maximum west-east extension of about 0.77 km. The eastern, southern and western shores of Dongdao Island are surrounded by 5–6-m-high sand barriers. The sand barrier on the southeastern shore is slightly higher than that on the northwestern shore. The sand barriers are covered with vegetation, dominated by *Scaevola sericea*, *Messerschmidia argentea*, *Guettarda speciosa* and *Aporosa villosa*. In the interior of this island is an up to 3 m high flat region, where about half the area is covered by *Pisonia grandis* woodland, providing a nesting place for numerous seabirds (Zhu et al. 2005). Under the *Pisonia grandis* woodland is black phosphoric soils enriched with organic matter. This island is presently occupied by approximately 35,000

breeding pairs of red-footed booby (*Sula sula*) (Cao et al. 2005), and it has been identified as the natural protection area for this seabird species.

"Cattle Pond" was discovered during our field investigations in 2003. It is a crescent-shaped fresh lake, located within the southwestern sand barrier with a height of 6 m. It is about 150 m long and has a maximum width of 15 m. The pond appears hydrologically closed, and the lake water is completely fed by atmospheric precipitation and lost predominantly through evaporation. At present, the water depth is usually less than 0.5 m, and varies with the alternation of dry and wet seasons. Field observation and geochemical studies showed that this pond is influenced significantly by seabird droppings (Liu et al. 2006).

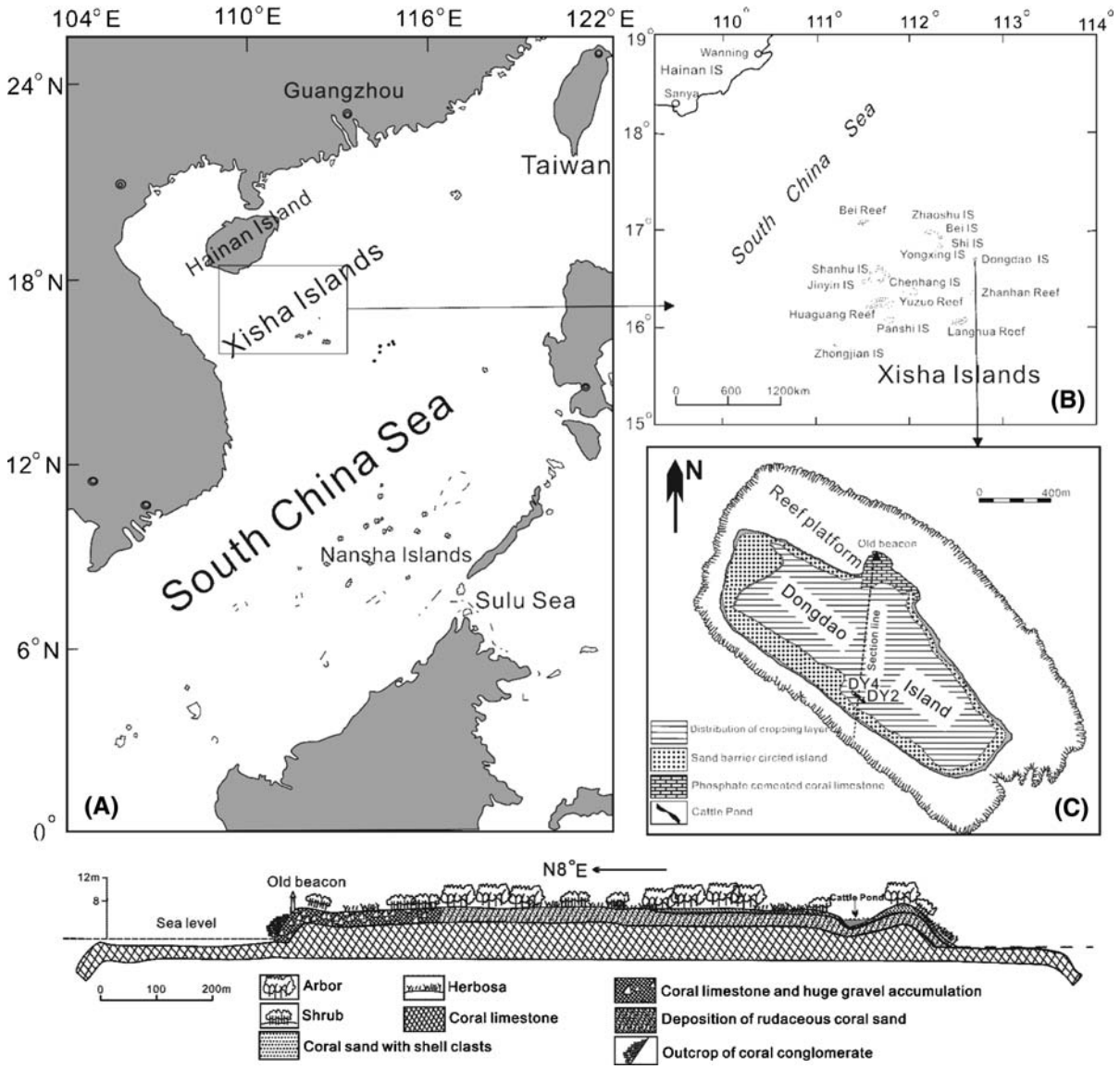

Fig. 1 Maps showing the geographic location of the study area (**A**), the Xisha Islands (**B**), Dongdao Island (**C**), and the distribution of morphological zones of Dongdao Island. Cattle Pond and sampling sites DY2 and DY4 are marked in figure (**C**). The bottom diagram is the section drawing of topography, vegetation, soils and parent materials along the section line from the old beacon to Cattle Pond, which is indicated in the top right figure (**C**)

Materials and methods

We collected two sediment cores from Cattle Pond (DY2 and DY4 of 126 and 117 cm long, respectively) using PVC plastic gravity pipes of 12 cm diameter. Sampling distance between the two coring sites was about 100 m. In the laboratory, the DY2 and DY4 cores were opened, photographed and described, and then sectioned at 1-cm intervals. Sediments of DY2 and DY4 contain abundant ostracodes and foraminifera, as well as caryopses of *Urochloa paspaloides*. Subsamples from both cores were analyzed for inorganic elemental concentrations, total organic carbon (TOC), total nitrogen (TN), total sulfur (TS), and loss on ignition at 550°C ($LOI_{550°C}$) and 950°C ($LOI_{950°C}$). Detailed analytical methods for these geochemical variables are found in Liu et al. (2006). The present study is mainly based upon data from DY4.

Ostracode valve occurrence in DY4 was inhomogeneous. When possible, we selected the best preserved adult valves for isotope analysis. A total of 56 monospecific ostracode (*Cyprinotus cingalensis*) valve samples were analyzed for oxygen and carbon isotopes. Handpicked shells were cleaned in a 5% H_2O_2 solution for 24 h to remove adhered organic matter, washed using high purity Milli-Q water, cleaned with ethanol, and then dried at room temperature. This process also removed adhered sand and silt sized grains.

The number of *Urochloa paspaloides* caryopses in the sediment of DY4 above 90 cm also exhibited notable fluctuations. These fossil seeds were well preserved in the ornithogenic sediments and were easily identified due to their large size ($\sim$2 mm in diameter) and picked out by hand using a bamboo toothpick. Caryopses were separated from the adhering sediments, and a total of 51 samples were selected. Before running organic carbon isotope analysis, we checked these caryopsis samples under the microscope to make sure they were monospecific and had consistent shape and structure.

The stable isotope compositions of carbon and oxygen in ostracode valves were analyzed using a GV IsoPrime® stable isotope ratio mass spectrometer (IRMS) coupled with an online carbonate preparation system (MultiPrep®) (Key Laboratory of Isotope Geochronology and Geochemistry, Guangzhou Institute of Geochemistry, CAS). Approximately 30 valves per sample of one species (*Cyprinotus cingalensis*) were selected to react with anhydrous phosphoric acid having a specific gravity of 1.92. Reaction occurred in a vacuum at a constant temperature of 90°C in an individual reaction vessel. Evolved gases were cryogenically purified to remove water and non-condensable gases. Purified CO_2 from the samples was introduced into the mass spectrometer through a capillary and measured against a reference standard of known isotopic composition. Organic carbon isotope analysis was performed on the plant remains using the off-line sealed tube combustion method (Liu et al. 2005a). Resultant CO_2 gas was then measured using a Finnigan-MAT 251 mass spectrometer.

Stable isotope abundances were expressed in δ notation as the deviation from standards in parts per thousand (‰) according to $\delta X = [(R_{sample}/R_{standard}) - 1] \times 1000$, where X is ^{13}C or ^{18}O and R is the corresponding ratio $^{13}C/^{12}C$ or $^{18}O/^{16}O$. The $R_{standard}$ values were based on the Vienna PeeDee Belemnite (V-PDB). For the measurement of ostracode isotope compositions, the mass spectrometer was calibrated with an internal carbonate standard (GBW04405), which has a composition of 0.57 ± 0.03 per mil and -8.49 ± 0.14 per mil for $\delta^{13}C$ and $\delta^{18}O$, respectively. Ten replicate analyses of this standard gave an external precision (1σ) better than 0.05‰ for $\delta^{13}C$ and 0.08‰ for $\delta^{18}O$. The average internal precision of $\delta^{13}C$ and $\delta^{18}O$ analytical results was 0.005‰ (1σ) and 0.006‰ (1σ), respectively. Replicate measurements of internal carbon black standard (GBW04407), which has an organic carbon isotope composition of -22.43 ± 0.07 per mil, indicate that the analytical precision of organic carbon isotopic measurement was within ±0.2‰, and the standard error between replicate samples (intervals with more than two replicates) was <0.4‰.

Element Ca and Mg analysis was performed on about 50 clean ostracode (*Cyprinotus cingalensis*) valves per sample. After dissolution in 3 ml of 0.5 mol/l HCl acid, the solution was analyzed for Ca and Mg using an Inductively Coupled Plasma Atomic Emission Spectrometer (ICP-AES). Based on the reproducibility analysis of five replicate samples, the mean relative error of the analyses was 3.8% for Mg/Ca.

Radiocarbon analyses for the DY4 core were performed solely on terrestrial organic matter (plant

Table 1 AMS ^{14}C dates and calibrated ages in sediment core DY4 from the Cattle Pond, on Dongdao Island

Laboratory number	Sample number	Dated material	Depth (cm)	^{14}C Conventional age (yr BP)	Calibrated age (cal yr BP)	
					Intercept	2 sigma
BA05842	DY4-21	Plant caryopsis	20–21	305 ± 40	417, 314, 411	474–289
BA05843	DY4-36	Plant caryopsis	35–36	765 ± 35	675	735–656
BA05844	DY4-45	Plant caryopsis	44–45	900 ± 35	790	924–730
BA051074	DY4-58(1)	Plant caryopsis	57–58	1,020 ± 30	932	970–804
BA051075	DY4-58(2)	Plant caryopsis	57–58	985 ± 30	926	953–794
BA051076	DY4-58(3)	Plant caryopsis	57–58	980 ± 30	925	951–793
BA051077	DY4-71(1)	Plant caryopsis	70–71	1,025 ± 30	933	971–917
BA051078	DY4-71(2)	Plant caryopsis	70–71	960 ± 30	916	945–790
BA051079	DY4-71(3)	Plant caryopsis	70–71	1,010 ± 40	930	972–795
BA051080	DY4-71(4)	Plant caryopsis	70–71	965 ± 30	919	947–790
BA05846	DY4-71(5)	Plant caryopsis	70–71	995 ± 35	928	966–794
BA05849	DY4-87	Plant caryopsis	86–87	1,340 ± 35	1,284	1,306–1,181

caryopsis). After HCl treatment, a total of 12 samples were determined using the Accelerator Mass Spectrometer facility at the Institute of Heavy Ion Physics in Peking University, and the resulting dates are reported with BA numbers assigned by this laboratory (Table 1). The AMS radiocarbon dates are expressed in conventional ^{14}C yr BP. The quoted errors in the dates are based on the reproducibility of measurement. The determined radiocarbon dates were then calibrated into calendar years before present (cal. BP) with the program OxCal version 4.3 and atmospheric data from Stuiver et al. (1998).

Results and discussion

Lithology and chronology

DY2 and DY4 have similar lithologies. Four sediment units were identified based on color, grain size and the presence of laminations (Fig. 2). The analysis of sedimentary facies showed that the bottom sediment units (Unit 4) of both cores consist of fragments of grey-white coral, shell and sandy gravels. These bottom sediments probably represent deposition in a lagoon environment, and they do not contain any ostracodes and plant remains. Above these sediments, both cores consist of ornithogenic sediments (Unit 2) with sharp stratigraphic contacts; the top 96 cm of DY2 and 87 cm of DY4 sediment layers contain considerable guano with the exception of the well-sorted coral sand layers (Unit 3) between 84–88 cm of DY2 and 58–69 cm of DY4. The ornithogenic sediments contain abundant ostracodes and caryopses of *Urochloa paspaloides*. The interbedded coral sand layer (Unit 3) has distinctly different lithology from the overlying and underlying sediments, and is not impacted by seabird droppings. The top 25 and 17 cm sediments (Unit 1) in DY2 and DY4 cores consist of brown-black humic mud enriched with plant remains. Abundant foraminifers were found throughout both cores, and they are mainly composed of benthic species including *Cibicides margaritifera*, *Baculogypsina* sp., *Rotaliids*, *Amphistegina* cf. *radiata* and *Poroeponides incrassatus*. These species are found in the coral sand layer in the Cattle Pond, indicating that these foraminifer remains did not originally inhabit this pond, but were likely transported by wind or water. One notable lithologic difference between DY2 and DY4 is that the top 25 cm sediment layer of DY2 contains lumpy cattle excreta, but we did not observe any cattle excreta in the top 17 cm sediment layer of DY4 (Liu et al. 2005b).

Profiles of $LOI_{950°C}$, CaO, $LOI_{550°C}$, TOC and TN in the DY2 and DY4 cores are plotted in Fig. 2 versus depth. $LOI_{950°C}$ reflects carbonate abundance, and $LOI_{550°C}$ indicates organic matter content (Liu et al. 2006). As shown in Fig. 2, TOC, TN, $LOI_{550°C}$, $LOI_{950°C}$ and calcium oxide (CaO) show sharp changes at 96 cm (DY2) and 87 cm (DY4). In the

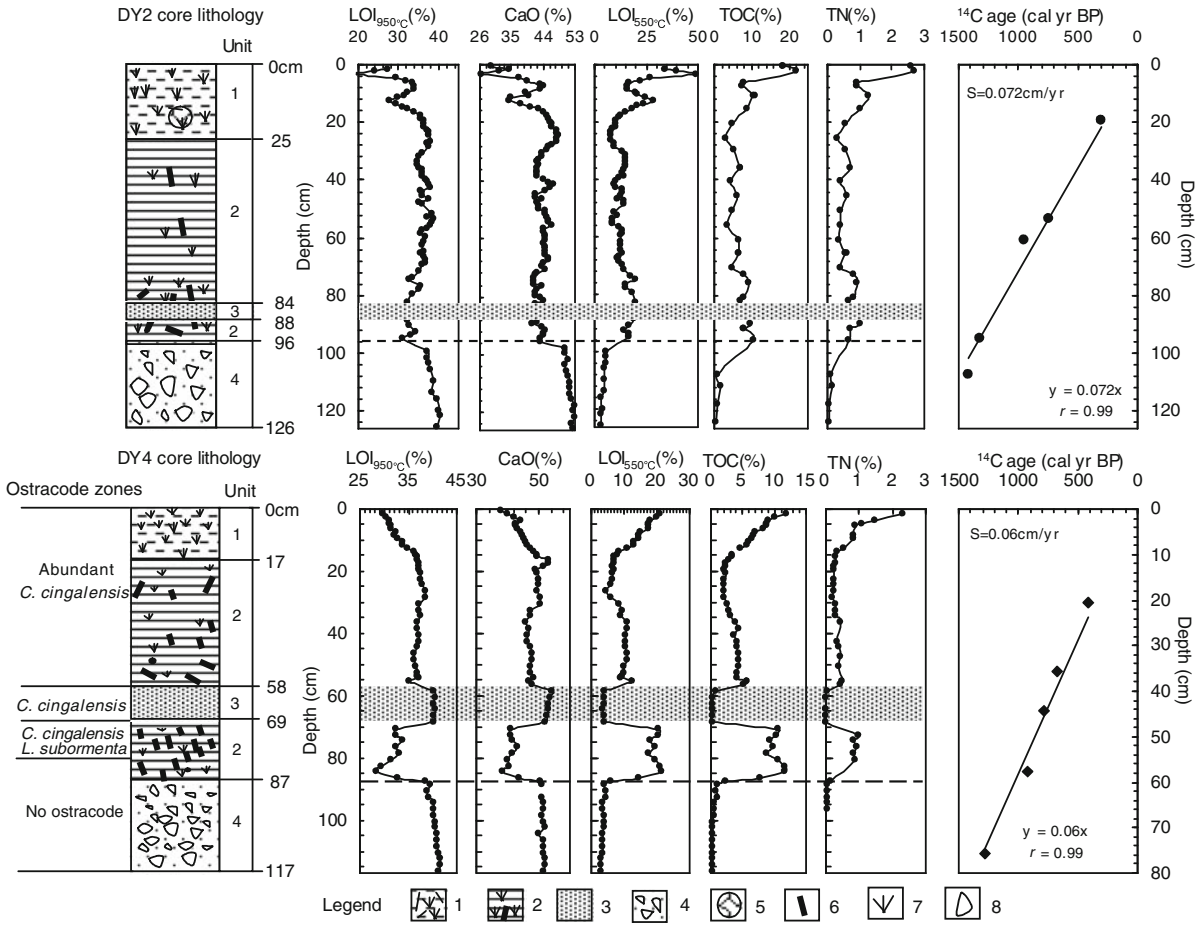

Fig. 2 Lithologic characteristics, down-core variation profiles of percent loss on ignition at 550 and 950°C, the contents of calcium oxide (CaO), total organic carbon (TOC) and total nitrogen (TN), and the age models for the DY2 and DY4 cores. Ostracode zones with characteristic species in the DY4 core are listed on the left. Legend: 1. Brown-black humic mud enriched with plant remains, containing seabird droppings. For sediment core DY2, lumpy cattle excreta are found at a depth of 19 cm. 2. Middle- to fine-grained coral sandy mud with brown-red color, containing seabird droppings; some yellow-white coral silts are intermingled in the sediments. 3. Well-sorted coral sand. 4. Grey-white coral, shell, and sandy gravel. 5. Lumpy cattle excrement. 6. Bones of seabirds and fish. 7. Remains of plant root and leaf. 8. Large coral clasts. Broken lines marked in the figure indicate the transition of sedimentary environment. The dotted area indicates the interbedded coral sand sediment layer with sharp stratigraphic contacts. A detailed discussion of the lithology and age model for the DY2 core is found in Liu et al. (2006)

sediments below these two critical points, the values of TOC, TN and $LOI_{550°C}$ are much lower than in those above; in contrast, the levels of $LOI_{950°C}$ and CaO are much higher. This is thought to represent change from an open lagoon characteristic of coral and shell clastic deposition (Unit 4) to a closed pond enriched with organic matter (Unit 2). The AMS ^{14}C dates suggested that this change occurred around 1,300 yr BP (Liu et al. 2006). Between 58 and 69 cm in DY4, $LOI_{950°C}$ and CaO display notable peaks, in contrast with the troughs of TOC, TN and $LOI_{550°C}$. This is apparently due to the dominance of well-sorted carbonate coral sand in Unit 3. Grain-size analyses, elemental geochemistry, and biological remains in the sediments showed that the interbedded coral sand layer (Unit 3, 84–88 cm of DY2 and 58–69 cm of DY4) possibly corresponds to a rapid marine sedimentation event, which is interpreted as extraordinary washover deposition associated with an intense typhoon or even tsunami (Sun et al. 2007). In sediment unit 1 above 17 cm in DY4 core, the values of TOC, TN and $LOI_{550°C}$ are relatively high (Fig. 2),

averaging 6.88% (n = 15), 0.95% (n = 9) and 13.95% (n = 16), likely reflecting the strengthened surface runoff that transported more materials rich in organic matter, such as herbaceous plants, leaves, guano, and surface humic soils, into the Cattle Pond. Similarly, the top 25 cm of DY2 also have the highest organic matter content. However, the change patterns of $LOI_{950°C}$, CaO, $LOI_{550°C}$, TN and TOC in the surface sediment layers of DY2 and DY4 are different. These variables show remarkable fluctuations in DY2, but not in DY4, and this seems to be caused by the variable input of cattle excreta into the upper 25 cm of DY2 (Sun et al. 2005). Overall, $LOI_{950°C}$, CaO, $LOI_{550°C}$, TOC and TN in the sediments of Cattle Pond mainly reflect the lithologic nature of the sediments. The vertical profiles of $LOI_{950°C}$ and CaO are opposite of those of $LOI_{550°C}$, TOC and TN, and this is explained by the dilution of organic matter input.

Ages of three and five plant caryopsis samples at depths of 57–58 cm and 70–71 cm in DY4 core, respectively, are consistent (Table 1). This suggests that the deposition of the interbedded coral sand layer between 58 and 69 cm was a sudden event and occurred around 926 cal yr BP, the average of eight AMS ^{14}C intercept ages with a mutual overlap of the 2 sigma ranges from 945 to 917 yr BP (Sun et al. 2007). When we converted sediment depths to age, this sediment depth should be excluded as it probably represents an abrupt event. The linear regression between depth and calibrated ^{14}C-age, excluding the interbedded sand layer, gave the equation: age (cal yr BP) = 0.06 × depth (cm) with an r of 0.99 and a sedimentation rate of 0.06 cm/yr. This sedimentation rate is similar to our previous result (~0.07 cm/yr), based on five AMS^{14}C dates on the bulk sediment organic matter in the DY2 core (Liu et al. 2006). On average, each 1-cm sample in DY4 represents about 16 years of sediment accumulation.

Ostracode species change

Some ostracodes are found in the lacustrine sediments above 80 cm in DY4 (~1,100 years before present), and results showed that the ostracode diversity is very low (Fig. 2). In sediments between 70 and 80 cm, the ostracode species are predominantly *Cyprinotus cingalensis* Brady and *Limnocythere subormenta* Hou. The former species has increasing abundance from 80 cm to 70 cm, and the latter has a decreasing one. A few ostracodes, mainly *Cyprinotus cingalensis*, occur in the coral sand layer between 58 and 69 cm. Above 58 cm, ostracodes are abundant, but they are exclusively *Cyprinotus cingalensis*. *Cyprinotus cingalensis* is usually found in either temporary pools with salinities up to 5‰ or in freshwater environments (Victor and Fernando 1981; De Deckker 1983). In contrast, *Limnocythere subormenta* predominantly inhabits brackish water and inland saltwater pools. The persistently increasing abundance of *Cyprinotus cingalensis* in the Cattle Pond may suggest decreasing salinity and a freshening trend over the past 1,100 years.

Oxygen and carbon isotopes in ostracode shells

Results show that the $\delta^{18}O$ values from the ostracode valves vary from −5.90‰ to −0.91‰ (Fig. 3). Because of the shallow water in the Cattle Pond, this range of ~5‰ in the $\delta^{18}O$ values may indicate relatively large variations in water composition and temperature during the calcification period of the adult carapaces, which usually occurs in the spring and fall (Xia et al. 1997; Schwalb and Dean 1998; Schwalb et al. 1999; Ricketts et al. 2001; Mischke et al. 2002). The $\delta^{13}C$ values in the valves also display large variation, ranging from −10.12 to −0.51‰. A cross plot of $\delta^{18}O_{ostracode}$ and $\delta^{13}C_{ostracode}$ (Fig. 3) shows that the ostracode valves form three populations: (1) in the top sediments above ~30 cm, (2) between 30 and 80 cm (except 58–69 cm), and (3) in the coral sand layer between 58 and 69 cm. The

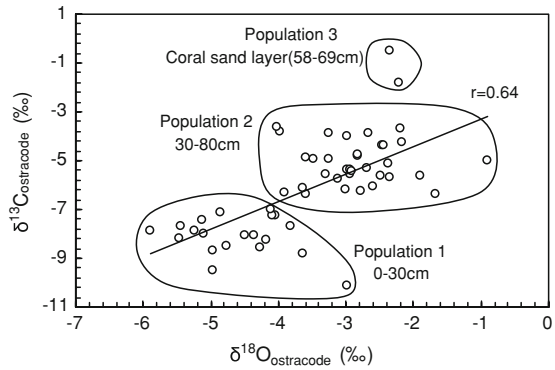

Fig. 3 Cross plot of $\delta^{13}C$ versus $\delta^{18}O$ data for the ostracodes taken from the sediment of core DY4. Linear fitting between two isotope values indicates a positive relationship

$\delta^{18}O_{ostracode}$ and $\delta^{13}C_{ostracode}$ in Population 2 ranges from −4.87 to −0.91‰ (averaging −2.91‰) and from −7.13 to −3.64‰ (averaging −5.19‰), respectively. Population 1 has relatively light isotope compositions: the values of $\delta^{18}O_{ostracode}$ vary from −5.90 to −2.98‰ with a mean of −4.57‰ and the $\delta^{13}C_{ostracode}$ values vary from −10.12 to −6.99‰ with a mean of −8.15‰. The ostracode valves extracted from the coral sand sediment layer (Population 3) have the highest $\delta^{13}C$ values. Considering population 1 and 2 as a whole, both oxygen and carbon isotope compositions in the ostracodes show a progressive shift to more negative values up core. A linear fitting shows that there is a positive correlation between $\delta^{18}O_{ostracode}$ and $\delta^{13}C_{ostracode}$ values (r = 0.64). The changes of $\delta^{18}O_{ostracode}$ and $\delta^{13}C_{ostracode}$ are plotted in Fig. 4 against depth or time. Values of $\delta^{18}O$ and $\delta^{13}C$ from ostracodes are highly variable, but in general they have a similar and overall decreasing trend through time.

Possible causes for large variations in $\delta^{18}O_{ostracode}$

The $\delta^{18}O$ of ostracode valves is dependent on the composition of the water in which the shells were formed, the temperature of formation, and vital effects (fractionation produced by the calcification). Interpretation of the $\delta^{18}O$ records requires a good

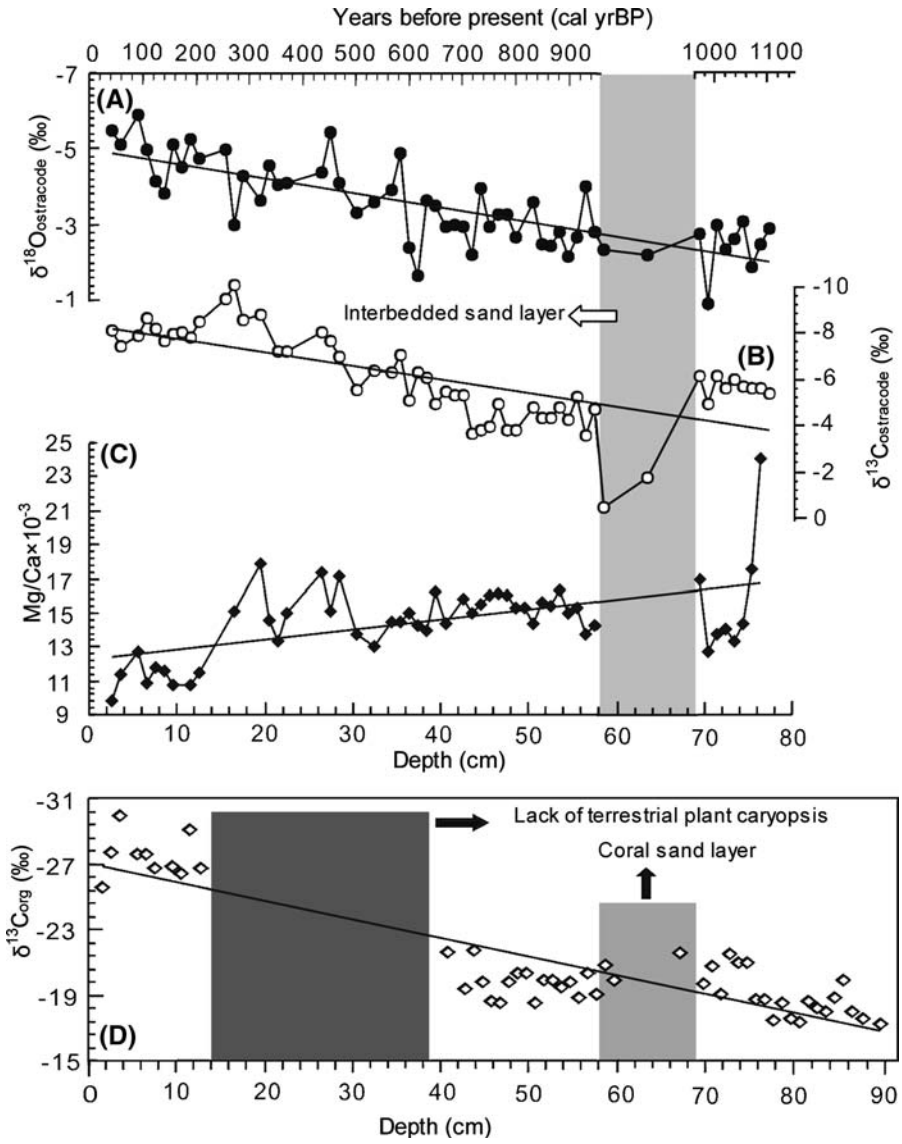

Fig. 4 $\delta^{18}O$ (**A**), $\delta^{13}C$ (**B**), Mg/Ca values (**C**) in the ostracode carbonate and organic $\delta^{13}C$ (**D**) in the caryopsis remains of *Urochloa paspaloides* in the sediment core DY4 versus age or depth. The first-order regression lines for each data set indicate a consistent trend towards more effective moisture over the last 1,100 years

understanding of these factors. The vital effect is a species specific, non-equilibrium fractionation process that preferentially incorporates one isotope of oxygen into the ostracode shell. In this study, almost a single species *Cyprinotus cingalensis* was usually analyzed to avoid problems associated with differences in individual species' vital effects (Ricketts et al. 2001).

The seasonal and long-term change of water temperature would influence the variation of $\delta^{18}O_{ostracode}$ values. Average monthly air temperatures in the Xisha Islands show an annual temperature range of about 5–6°C and vary between 23.1 and 29.1°C. Seasonal variation in lake water temperature could cause up to 1.5‰ difference among ostracodes from one stratigraphic level, not sufficient to cause the observed larger variations in the $\delta^{18}O$ values in the ostracode valves of Cattle Pond. Moreover, the samples for isotope analyses consisted of multiple ostracode valves, and this should average out seasonal variations. The $\delta^{18}O$ values in ostracode valves are correlated negatively with temperature (ca. −0.24‰ per °C) and correlated positively with oxygen-isotope composition of the host water (Stuiver 1970). Assuming that the observed $\delta^{18}O$ fluctuations are mainly caused by water temperature and that the rate of decrease of $\delta^{18}O$ is 0.24‰ per 1°C, the range of ∼5‰ in $\delta^{18}O$ would correspond to a temperature change of 21°C over the past 1,100 years. Such large temperature variation is neither realistic for tropical lake water conditions nor for the normal living conditions of ostracode species. Furthermore, according to the sea surface temperature (SST) reconstructed from coral in the northern coast of the South China Sea, variations in summer, winter, and annual average SST were less than 3°C since the Mid-late Holocene (Wei et al. 2004; Yu et al. 2005), i.e. <1‰ in the $\delta^{18}O$ value in ostracode shells.

The oxygen isotope composition of ostracode shells is also controlled by the isotopic composition of the lake water in which the shells are formed. The variations in oxygen isotope abundance ratios of lake water depend upon the changes in the isotopic composition of precipitation, in the precipitation/evaporation balance, and the hydrologic conditions in the basin (evapotranspiration, hydrologic changes) (Filippi et al. 1999). Closed-basin lakes generally lose a significant fraction of their water to evaporation. In the tropical Xisha Islands, due to high solar insolation and temperature (mean annual temperature = 26–27°C), evaporation effect is very strong. Annual evaporation is up to about 2,400 mm, much more than annual precipitation (∼1,500 mm), and this leads to relatively dry climate in this region. Under these climatic conditions, we speculate that evaporation could have had significant effect on the isotope composition of lake water, although this hypothesis needs to be verified by the isotope composition of multiple water samples. Evaporation preferentially removes water containing ^{16}O from a water body due to its higher vapor pressure, and thus increases the $\delta^{18}O$ composition of residual lake water. The soil water and guano phosphoric deposits on tropical islands display obvious ^{18}O enrichment relative to meteoric water, confirming the existence of a well-developed evaporation profile (Ayliffe et al. 1992; Liu et al. 2008). The magnitude of this fractionation effect is controlled by the temperature and relative humidity of the atmosphere at which evaporation occurs, as well as wind speed, solar radiation, and atmospheric radiation (Hostetler and Benson 1994). Cattle Pond is a very shallow and hydrologically closed lake, and the $\delta^{18}O$ of the ostracode shells from this lake is expected to be primarily affected by the isotope composition and amount of precipitation and the degree of evaporation in response to changing hydrologic balance.

Cattle Pond receives predominantly local ground water flow. Because of the very short distance the water travels to flow into the pond, the isotope composition of local ground water flow without significant evaporation should be very close to that of local precipitation. The isotopic composition of atmospheric precipitation is geographically and temporally specific, and is controlled by a series of fractionation processes, including evaporation from source, condensation, and precipitation. A worldwide survey of monthly $\delta^{18}O$ values of precipitation initiated by IAEA and WMO in 1961 observed empirical relationships between the isotopic composition of precipitation and several geographic effects (Bowen and Wilkinson 2002). The isotopic ratio of precipitation at any one locality through time depends on the source of the moisture and the air-mass trajectory. Although the climate on Dongdao Island is influenced by two different air masses, only the southwest monsoon air mass contributes a significant amount of moisture to the island. A single moisture

source cannot result in a notable shift in isotope signature of precipitation in a systematic way. Aggarwal et al. (2004) suggested that the stable isotope composition of groundwater from the Asia monsoon region had almost no variation from the Last Glacial Maximum (LGM) to present, and the overall structure of the monsoon circulation systems and moisture transport patterns, which are governed primarily by the movements of the Intertropical Convergence Zone (ITCZ), were likely the same during the LGM as observed today.

Recently, the "amount effect" was proposed to describe the inverse relationship between the amount and the isotope composition of precipitation. The effect is greatest in tropical areas of monsoon activity (Zhang et al. 2004; Ichiyanagi and Yamanaka 2005; Vuille et al. 2005; Brown et al. 2006). The monthly and annual isotope signal measured on tropical islands should be dominated by the amount effect. Dongdao Island is strongly influenced by summer monsoon precipitation, and the $\delta^{18}O$ in precipitation should be strongly related to the amount of precipitation. An increase in precipitation amount should produce more negative $\delta^{18}O$ of rainfall, and thus a decrease in $\delta^{18}O$ composition of the water in Cattle Pond. Depletion in the abundance of ^{18}O is well documented from tropical cyclones. According to Lawrence and Gedzelman (1996), tropical cyclone rains have $\sim$6.5‰ lower oxygen isotope ratio than rain in other tropical and summer precipitation systems. Thus, isotope analysis of ancient fresh water fossil carbonate shells, fossil mammal teeth, or tree rings might be used to document past tropical cyclone activity (Lawrence 1998).

In summary, Cattle Pond reacts sensitively and quickly to changes in effective moisture, and the $\delta^{18}O$ values of the ostracode valves in Cattle Pond are very likely controlled by the changes in evaporation vs. precipitation (effective moisture). The trend towards lower oxygen-isotope values indicates an increase in effective moisture and thus increased frequency of storm events, amount of precipitation, and/or decreased evaporation.

Possible causes for large variations in $\delta^{13}C_{ostracode}$

Changes in the ostracode-inferred $\delta^{13}C$ values of lake water can be influenced by various factors including: (1) the dissolved inorganic carbon (DIC) pool in near-surface waters, depleted in ^{12}C by algal productivity; (2) particulate organic carbon (POC), dissolved organic carbon (DOC), particulate inorganic carbon (PIC) and DIC in bottom waters enriched with ^{12}C from the degradation of organic matter; (3) terrestrial vegetation cover and change (C3 vs. C4, abundant vs. sparse vegetation and its effect on the amount of soil respiration); and (4) exchange between atmospheric CO_2 and DIC of lake water (Xia et al. 1997; Mischke et al. 2002).

For carbon isotopes, the temperature fractionation effect for calcite or aragonite is much lower than that for oxygen isotopes (Mischke et al. 2002; Schwalb and Dean 1998), and the range of $\delta^{13}C$ values in the ostracode calcite from Cattle Pond cannot be explained in terms of water temperature.

Photosynthesizing organisms utilize ^{12}C preferentially, leaving surface water DIC relatively enriched in ^{13}C. At the lake bottom, isotopically light carbon is released through degradation of organic matter and recycled by ostracodes and other benthic carbonate-shelled organisms. Increased productivity in the surface waters leads to relatively negative composition in oxic bottom waters, thereby decreasing the carbon isotope composition of the ostracode shells formed on the sediment/water interface. The above hypotheses have been widely used to explain stratigraphic shifts of $\delta^{13}C$ in ostracode valves (Ricketts et al. 2001; Schwalb and Dean 2002; Schwalb et al. 2002; Schwalb 2003). In Cattle Pond, although there is abundant nutrient input from seabird droppings and recent cattle excrement, biological productivity and/or eutrophication processes may have negligible impact on the isotope composition variations in the ostracodes. First, according to our field observation, productivity of Cattle Pond is very low due to its shallow water and propensity to drying; the organic matter deposited in Cattle Pond originated mainly from external sources such as plants, leaves, guano, and surface humic soils within the catchment. This finding is supported by the result of our previous study on the carbon and nitrogen isotope compositions of sedimentary bulk organic matter and the sediment organic geochemistry (Liu et al. 2005b; Wang 2007). Second, phosphorus, predominantly derived from seabird droppings, has a significant and positive correlation with organic matter in the ornithogenic sediment layers of DY2 (except for the top 25 cm sediments) and DY4 (Liu et al. 2006).

Since the land humus is crucial for the liberation of phosphate from guano and for the enhancement of phosphate mobility in many natural aqueous systems, terrestrially-derived guano might account for a large proportion of organic sediments in the Cattle Pond. Therefore, in Cattle Pond, the increase in the TOC and TN (Fig. 2) may not indicate an increase in organic productivity, but more likely it is simply the result of a marked decrease in dilution by coral sand material (possibly due to the well-vegetated island). The $\delta^{13}C_{ostracode}$ values have no correlation with the phosphorus content and TOC, TN values. Third, based on the carbon isotope data in plants around Cattle Pond (Liu et al. 2005b), C3 plants are dominant relative to C4 plants. Therefore, the $\delta^{13}C_{ostracode}$ variation is unlikely caused by a change in the relative abundance of C3 versus C4 plants in the catchment. Last, stable isotope composition in the ostracodes is generally influenced by primary productivity in lakes. As will be discussed below, however, the Mg/Ca ratios in the ostracode valves and the organic carbon isotope in the monospecific caryopses are not controlled by lake productivity, but they display similar change patterns versus depth or age. Thus, the $\delta^{13}C$ in the ostracodes of Cattle Pond is more likely controlled by the changes in climatic conditions rather than lake productivity.

Exchange with the atmosphere will cause a lake's DIC pool to equilibrate with atmospheric CO_2. Since the fractionation factor between dissolved bicarbonate and CO_2 is 8–10‰ (5–25°C) and the composition of atmospheric CO_2 is −7‰, lake water DIC equilibrated with the atmosphere would have a composition between +1 and +3‰ (Ricketts et al. 2001). However, Cattle Pond is too shallow to stratify, lake waters are well mixed, and the CO_2 in the water can be exchanged completely with the atmosphere. The contribution of atmospheric CO_2 (less negative source) to the lake water should not change significantly through time, thus the influence of CO_2 exchange on the variations in $\delta^{13}C_{ostracode}$ was probably negligible.

With increased or decreased freshwater input to cattle Pond, the $\delta^{13}C$ composition of the lake water may rise or fall depending on the input carbon sources, i.e., the mineralized organic matter and the dissolution of carbonate coral sand. Therefore, the $\delta^{13}C$ values in the ostracode valves are very likely affected by two isotopically distinct sources of carbon: terrestrial organic material via oxidized guano and soil organic matter with ^{13}C depletion, and weathered carbonate coral sand enriched with ^{13}C. Terrestrial organic matter in the environmental samples around Cattle Pond has relatively low $\delta^{13}C$ values (Liu et al. 2005b): the guano has an average $\delta^{13}C$ value of −22‰ (n = 3); most plants growing around Cattle Pond, surface humic soils, and cattle excrement have $\delta^{13}C$ values in the range of −26 to −29‰ (n = 6); The $\delta^{13}C$ values in the sedimentary organic matter of Cattle Pond vary from −21 to −29‰ (n = 24). The Cattle Pond has a pH of 8–10, likely due to the high carbonate content in the lacustrine sediment (Liu et al. 2006). Under this condition, HCO_3^- is generally the dominant carbon species in lake water. Isotopically light CO_2 (around −22 to −29‰) from decayed terrestrial organic matter and guano could enter soil water and shallow ground water, which finally flows into Cattle Pond. Resultant HCO_3^- should have $\delta^{13}C$ values of −12 to −19‰ based on the isotope fractionation equation that shows HCO_3^- in equilibrium with CO_2 gas has $\delta^{13}C$ values ~10‰ higher than CO_2 (Leng and Marshall 2004). The decay of organic matter releases ^{13}C-depleted CO_2 to the lake water where it is taken up by benthic ostracodes (Mischke et al. 2002), leading to relatively low carbon isotope compositions in the ostracode shells. On the other hand, the ground surface of Dongdao Island is covered with abundant coral sand, and the carbon isotopic composition of these carbonate materials is generally in equilibrium with that of sea water and has relatively high $\delta^{13}C$ values (Trichet and Fikri 1997). Interestingly, the ostracode valves extracted from the coral sand sediment layer between 58 and 69 cm of DY4 have $\delta^{13}C$ values of about 0‰, close to those of modern surface seawater (+1.5 ± 0.8‰) (Kroopnik 1985), but much higher than those in other sediments. This indicates that the carbon pool in the coral sand layer was mainly derived from a sea source, consistent with our previous results that the interbedded coral sand layer of DY4 came from a sudden marine sedimentation event.

All the $\delta^{13}C$ values in the ostracode shells of Cattle Pond vary between those of coral sand and organic matter (Fig. 4). Therefore, the change in $\delta^{13}C_{ostracode}$ composition in DY4 can be explained as the shift in the contribution from two distinct carbon sources. The decreasing tendency of $\delta^{13}C$ values in

the ostracode valves from the bottom to top represents an increasing decay of organic matter and runoff, and the increasing decay may be related to, as indicated by $\delta^{18}O$ changes, increasing precipitation. Groundwater in the wetter catchment of Cattle Pond is more influenced by decomposition of ^{13}C-depleted organic matter than groundwater of drier, thinly vegetated catchments. Therefore, an increase in effective moisture would result in a decrease in $\delta^{18}O$ composition of lake water; at the same time it would lead to more intensive decomposition of guano and plants, a rise in the supply of ^{13}C-depleted CO_2 to ground water and Cattle Pond, and finally a reduction of the $\delta^{13}C_{ostracode}$ values in the sediments of Cattle Pond.

Mg/Ca ratios in ostracode valves

The general trend of increasing effective moisture is also supported by the change of Mg/Ca ratios in the ostracode valves. As shown in Fig. 4, the Mg/Ca ratios in the ostracode shells showed remarkable variation, ranging from 0.01 to 0.024, and a shift toward much lower Mg/Ca ratios in the upper samples. The Mg/Ca of ostracode calcite is generally considered to be controlled by both Mg/Ca in ambient waters and temperature (Chivas et al. 1986; Ricketts et al. 2001). With regard to the present Cattle Pond, the slight change of water temperature, as discussed above, unlikely caused significant change in Mg/Ca ratios of the ostracode valves. The large change of ostracode Mg/Ca should be controlled mainly by the ionic ratios in the host water. In the closed Cattle Pond, evaporative concentration of lake waters could lead to increases in salinity, causing high Mg/Ca ratio in the lake waters. The long-term trend toward lower Mg/Ca ratios (Fig. 4) indicates a decrease in salinity over the past 1,100 years, corresponding to an increasing trend of effective moisture.

Organic carbon isotopes in caryopses (*Urochloa paspaloides*)

A long-term trend toward more effective moisture recorded in the ostracode shells is further supported by the change in organic $\delta^{13}C$ values of the well preserved caryopsis remains of *Urochloa paspaloides* in the lacustrine sediments. There are no organic $\delta^{13}C$ data for the sediments between 15 and 40 cm (corresponding to $\sim$1400–1850 AD) since we did not find enough plant caryopses therein. The reason for their absence is still unclear, and it may be due to the relatively cool climate during the Little Ice Age (LIA) (Liu et al. 2007). The $\delta^{13}C$ values of the caryopses in the upper 14 cm sediment layer were around $-27‰$, significantly lower than -17 to $-22‰$ of the caryopses below 40 cm (Fig. 4).

Based on plant physiology, Francey and Farquhar (1982) reported that the $\delta^{13}C$ composition of plants is a function of atmospheric CO_2 concentration, photosynthetic rate, and stomatal conductance. The latter two factors are considered to be strongly related to climatic variables such as temperature, humidity, precipitation, solar radiation and wind. The upper 14 cm of sediment in DY4 covered a time period of about 220 years, the time of burning of fossil fuels. The significant increase of atmospheric CO_2 concentration could result in a negative shift in the atmospheric $^{13}C/^{12}C$ ratio. However, according to numerous studies of tree rings and ice cores, the change in $\delta^{13}C$ values of the atmospheric CO_2 was less than 1–2‰ (Freyer and Belacy 1983; Leavitt and Lara 1994; Francey et al. 1999). Thus, this factor could not have contributed significantly to the variation of $\delta^{13}C$ values in the caryopses.

Water and salinity stress could have had a substantial effect on plant photosynthesis. *Urochloa paspaloides* is an annual herb, and the period of flowering and fruiting is May–October. This plant species generally grows around the lake or on the mountain slopes, and water availability is an important factor for its growth. Fresh groundwater on Dongdao Island is very scarce due to its small land area and low elevation. Moreover, water-retention by the coral sandy soil is very poor because of its coarse texture and high porosity, and water for plant growth is mainly from atmospheric precipitation and subsurface water. To make the matter worse, high rates of evaporation and short, intense convective rainfall events tend to restrict moisture for plant growth. Water stress is therefore a key limiting factor for plant growth in this coral island. In order to reduce water transpiration, most plants on Dongdao Island exhibit the eurybiontic behavior. They are tolerant of high salinity and adapted to aridity (Zhang 1974). The increase in precipitation would result in relatively higher humidity and water content in the surface soil, a decrease in water stress for plant

growth, and a reduction in the salinity of the soil. Many investigations have demonstrated that environmental factors, particularly growth-limiting factors, are generally responsible for isotope fractionation observed in plants. The combination of increasing moisture and decreasing salinity would enhance photosynthetic capacity and stomatal conductance, and the resultant interior CO_2 concentration would finally result in a decrease of $\delta^{13}C$ values in plants (Ma et al. 2005; Li et al. 2007). Therefore, the remarkable decrease of the organic $\delta^{13}C$ values in the caryopsis remains of DY4 indicates a substantial increase in effective moisture.

What caused the progressive increase in effective moisture on Dongdao Island? We suggest two possible scenarios. First, the climate in this area may have changed over the last 1,100 years. The reconstructed climatic temperatures for China and the Northern Hemisphere are in good agreement over the past millennium (Yang et al. 2002), and they display natural trends toward cooling climate, except for the 20th century. The relatively high temperature of the recent century and the departure from the natural cooling trend is believed to be related to global warming in response to the increases in anthropogenic greenhouse gases. Reconstructed temperatures indicate relatively warm hemispheric conditions earlier in the millennium (Medieval Warm Period), and the cooling following the 14th century could be viewed as the initial onset of the Little Ice Age due to the effect of astronomical forcing (Mann et al. 1999). As previously shown, Dongdao Island is located in a drought-sensitive area, with a net water deficit of ~900 mm/yr. The long-term cooling trend over the past 1,000 years may have reduced evaporation. A decrease in evaporative loss may have resulted in a progressive increase in effective moisture in Cattle Pond. Nevertheless, in contrast with recent global warming, the reconstructed effective moisture on Dongdao Island still displays an increasing trend over the past 100 years.

Another possibility is that a change in tropical cyclones may have changed the precipitation. As shown in Fig. 5, there is a statistically positive correlation between the instrumentally measured precipitation and observed tropical cyclone frequency over the past four decades. Since the time resolution of lacustrine sediments of DY4 core is relatively low, about 16 years per 1 cm sediment thickness, we could not examine the direct correlation between proxy records of stable isotope and trace element compositions and modern meteorological data. Assuming a similar correlation between hydrology and tropical cyclone frequency for the past 1,100 years (a reasonable assumption), the relative variation in effective moisture, as recorded in ostracode valves and caryopsis remains of DY4, could be used as an indirect indicator of the change in tropical cyclone frequency; and the long-term trend toward more effective moisture may suggest a persistent increase of tropical cyclone frequency in the Xisha area of the South China Sea over the past 1,100 years.

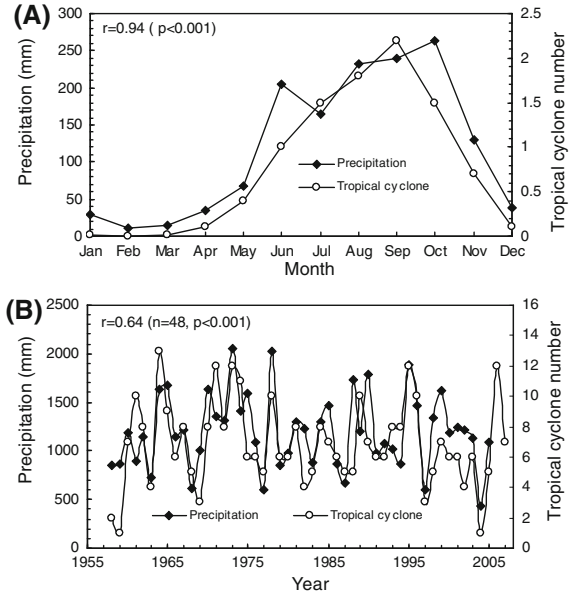

Fig. 5 Monthly (**A**) and annual (**B**) precipitation and cyclone number in the Xisha area during 1958–2005. The monthly number of tropical cyclones used in the upper figure (**A**) was those formed in the west part of South China Sea (14–23°N, 105–115°E) during 1958–1994 (Wang 1998), and the annual cyclone number in the bottom figure (**B**) during 1995–2005 was counted from the web database (http://weather.unisys.com/hurricane/), based on the criterion that the tropical cyclones passed within 500 km of Dongdao Island

In recent years, numerous studies have addressed the issue of tropical cyclone frequency in the South China Sea based on instrumental data. Because of the short time scale, these studies argued that the variability of tropical cyclone frequency did not display a discernible trend over the past 50 years (Chan and Shi 1996; Wang et al. 2006). If the hypothesis that the change in effective moisture on Dongdao Island is related to the frequency of tropical

cyclones is right, then our long-term data on isotope composition in hydrologically-closed Cattle Pond, South China Sea, permits us to infer an increasing frequency of tropical cyclones for the past 1,100 years. Since these variations occurred before the industrial revolution, natural factors apparently played a dominant role in the climate change. The actual cause of tropical cyclone and precipitation variations, however, may only be revealed with further study.

Conclusions

Dongdao Island (16°39′–16°41′ N, 112°43′–112°45′ E) is located in the eastern sector of the Xisha Islands, South China Sea. According to modern meteorologic data, there exists a statistically positive correlation between instrumentally measured precipitation, both monthly and annually, and observed tropical cyclone activity over recent decades. Tropical cyclone-induced precipitation may account for a significant portion of total annual precipitation on Dongdao Island. Results from analyses of oxygen and carbon isotopes and elemental analyses (Ca and Mg) on sediment core DY4 from Cattle Pond, on Dongdao Island, showed increasing effective moisture and rainfall intensity over the past 1,100 years. A possible explanation for the increasing trend of effective moisture is an increase in tropical cyclone frequency. However, this study is only based on a single core from Dongdao Island, and the presumed correlation between proxy data and tropical cyclone frequency is tentative. In order to better understand the long-term dynamics of climate in this region, further research is necessary, requiring the study of lake water samples, and high-resolution proxy records of sediment cores from other islands in the South China Sea.

Acknowledgements This research was supported by grants from the key project of the National Natural Science Foundation of China (No. 40730107 and 40606003), the Projects of the Knowledge Innovation of CAS (No. KZCX3-SW-151) and Cooperative Foundation from Key Laboratory of Isotope Geochronology and Geochemistry, CAS. We are grateful to the P. R. China Military for authorizing us to perform the research project in Xi-Sha atoll and to P. R. China troops in Xi-Sha atoll for their sampling assistance. We are also grateful to Prof. Dahe Qin and Prof. Lingen Bian at China Meteorological Administration for their constructive suggestion and providing modern meteorologic data in the Xisha area, Prof. Zhouqing Xie, Dr. Xuebin Yin, Sanping Zhao for the assistance with fieldwork sampling, and Prof. Shoubiao Zhou at Anhui Normal University for the identification of caryopsis species taken from the lacustrine sediments. We especially appreciate Dr. Antje Schwalb and one anonymous reviewer for their constructive review comments and suggestions, and Dr. Mark Brenner for improving English usage.

References

Aggarwal PK, Fröhlich K, Kulkarni KM, Gourcy LL (2004) Stable isotope evidence for moisture sources in the Asian summer monsoon under present and past climate regimes. Geophys Res Lett 31:L08203. doi:10.1029/2004GL019911

Anadón P, Moscariello A, Rodríguez-Lázaro J, Filippi ML (2006) Holocene environmental changes of Lake Geneva (Lac Léman) from stable isotopes ($\delta^{13}C$, $\delta^{18}O$) and trace element records of ostracod and gastropod carbonates. J Paleolimnol 35:593–616

Ayliffe LK, Veeh HH, Chivas AR (1992) Oxygen isotopes of phosphate and the origin of island apatite deposits. Earth Planet Sci Lett 108:119–129

Bahr A, Arz HW, Lamy F, Wefer G (2006) Late glacial to Holocene paleoenvironmental evolution of the Black Sea, reconstructed with stable oxygen isotope records obtained on ostracod shells. Earth Planet Sci Lett 241:863–875

Bowen GJ, Wilkinson B (2002) Spatial distribution of $\delta^{18}O$ in meteoric precipitation. Geology 30:315–318

Brown J, Simmonds I, Noone D (2006) Modeling $\delta^{18}O$ in tropical precipitation and the surface ocean for present-day climate. J Geophys Res 111(D5):D05105. doi:10.1029/2004JD005611

Cao L, Pang YL, Liu NF (2005) Status of the Red-Footed Booby on the Xisha Archipelago, South China Sea. Waterbirds 28:411–419

Chan JCL Shi JE (1996) Long-term trends and interannual variability in tropical cyclone activity over the western North Pacific. Geophys Res Lett 20:2765–2767

Chivas AR, De Deckker P, Shelley JMG (1986) Magnesium content of nonmarine ostracod shells: a new palaeosalinometer and palaeothermometer. Palaeogeogr Palaeoclimatol Palaeoecol 54:43–61

De Deckker P (1983) Notes on ecology and distribution of non-marine ostracods in Australia. Hydrobiologia 106: 223–234

Dettman DL, Palacios-Fest MR, Nkotagu HH, Cohen AS (2005) Paleolimnological investigations of anthropogenic environmental change in Lake Tanganyika: VII. carbonate isotope geochemistry as a record of riverine runoff. J Paleolimnol 34:93–105

Donnelly JP, Woodruff JD (2007) Intense hurricane activity over the past 5,000 years controlled by El Niño and the West African monsoon. Nature 447:465–468

Donnelly JP, Roll S, Wengren M, Butler J, Lederer R, Webb T (2001) Sedimentary evidence of intense hurricane strikes from New Jersey. Geology 29:615–618

Emanuel K (2005) Increasing destructiveness of tropical cyclones over the past 30 years. Nature 436:686–688

Filippi ML, Lambert P, Hunziker J, Kűbler B, Bernasconi S (1999) Climatic and anthropogenic influence on the stable isotope record from bulk carbonates and ostracodes in Lake Neuchatel, Switzerland, during the last two millennia. J Paleolimnol 21:19–34

Francey RJ, Farquhar GD (1982) An explanation of $^{13}C/^{12}C$ variations in tree rings. Nature 297:28–31

Francey RJ, Allison CE, Etheridge DM, Trudinger CM, Enting IG, Leuenberger M, Langenfelds RL, Michel E, Steele LP (1999) A 1000-year high precision record of $\delta^{13}C$ in atmospheric CO_2. Tellus 51B:170–193

Freyer HD, Belacy N (1983) $^{13}C/^{12}C$ records in northern hemispheric trees during the past 500 years: anthropogenic impact and climatic superposition. J Geophys Res 88:6844–6852

Hostetler SW, Benson LV (1994) Stable isotopes of oxygen and hydrogen in the Truckee River-Pyramid Lake surface-water system. 2. A predicitive model of $\delta^{18}O$ and $\delta^{2}H$ in Pyramid Lake. Limnol Oceanogr 39:356–364

Hoyos CD, Agudelo PA, Webster PJ, Curry JA (2006) Deconvolution of the factors contributing to the increase in global hurricane intensity. Science 312:94–97

Ichiyanagi K, Yamanaka MD (2005) Interannual variation of stable isotopes in precipitation at Bangkok in response to El Niño Southern Oscillation. Hydrol Process 19: 3413–3423

Kroopnik P (1985) The distribution of CO_2 in the world oceans. Deep Sea Res 32:57–84

Lambert WJ, Aharon P, Rodriguez AB (2008) Catastrophic hurricane history revealed by organic geochemical proxies in coastal lake sediments: a case study of Lake Shelby, Alabama (USA). J Paleolimnol 39:117–131

Landsea CW (2005) Hurricanes and global warming. Nature 438:E11–E13

Lawrence JR (1998) Isotopic spikes from tropical cyclones in surface waters: opportunities in hydrology and paleoclimatology. Chem Geol 144:153–160

Lawrence JR, Gedzelman SD (1996) Low stable isotope ratios of tropical cyclone rains. Geophys Res Lett 23:527–530

Leavitt SW, Lara A (1994) South American tree rings show declining $\delta^{13}C$ trend. Tellus 46B:152–157

Leng MJ, Marshall JD (2004) Palaeoclimate interpretation of stable isotope data from lake sediment archives. Quat Sci Rev 23:811–831

Li YB, Chen T, Zhang YF, An LZ (2007) The relation of seasonal pattern in stable carbon compositions to meteorological variables in the leaves of *Sabinaprzewalskii* Kom. and *Sabina chinensis* (Lin.) Ant. Environ Geol 51: 1279–1284

Liu KB, Fearn M (2000) Reconstruction of prehistoric landfall frequencies of catastrophic hurricanes in Northwestern Florida from lake sediment records. Quat Res 54:238–245

Liu XD, Sun LG, Yin XB, Zhu RB, Xie ZQ, Wang YH (2005a) A preliminary study of elemental geochemistry and its potential application in Antarctic seal palaeoecology. Geochem J 39(1):47–59

Liu XD, Sun LG, Zhao SP, Yin XB, Xie ZQ, Luo HH (2005b) Eco-environmental information recorded in the lake sediments of Dongdao Island, South China Sea. Quat Sci 25:574–584 (in Chinese with English abstract)

Liu XD, Zhao SP, Sun LG, Luo HH, Yin XB, Xie ZQ, Wang YH, Liu KX, Wu XH, Ding XF, Fu DB (2006) Geochemical evidence for the variation of historical seabird population on the Dongdao Island of South China Sea. J Paleoliminol 36:259–279

Liu XD, Sun LG, Wang JJ, Zhao SP, Liu KX, Wu XH (2007) Eco-environment response to climate changes on Dongdao Island of South China Sea over the past 1300 years. J Univ Sci Technol China 37(8):1009–1016 (in Chinese with English abstract)

Liu XD, Sun LG, Cheng ZQ, Zhao SP, Liu KX, Wu XH, Xie ZQ, Yin XB, Luo HH, Ding XF, Fu DB, Wang YH (2008) Paleoenvironmental implications of the guano phosphatic cementation on Dongdao Island in the South China Sea. Mar Geol 247:1–16

Ma JY, Chen T, Qiang WY, Wang G (2005) Correlation between foliar stable carbon isotope composition and environmental factors in desert plant Reaumuria Soongorica (Pall.) Maxim. J Integr Plant Biol 47:1065–1076

Mann ME, Bradley RS, Hughes MK (1999) Northern hemisphere temperatures during the past millennium: inferences, uncertainties, and limitations. Geophys Res Lett 26:759–762

Mischke S, Fuchs D, Riedel F, Schudack ME (2002) Mid to Late Holocene palaeoenvironment of Lake Eastern Juyanze (north-western China) based on ostracods and stable isotopes. Geobios 35:99–110

Nott J (2004) Palaeotempestology: the study of prehistoric tropical cyclones – a review and implications for hazard assessment. Environ Int 30:433–447

Ortiz JE, Torres T, Delgado A, Reyes E, Llamas JF, Soler V, Raya J (2006) Pleistocene paleoenvironmental evolution at continental middle latitude inferred from carbon and oxygen stable isotope analysis of ostracodes from the Guadix-Baza Basin (Granada, SE Spain). Palaeogeogr Palaeoclimatol Palaeoecol 240:536–561

Ricketts RD, Johnson TC, Brown ET, Rasmussen KA, Romanovsky VV (2001) The Holocene paleolimnology of Lake Issyk-Kul, Kyrgyzstan: trace element and stable isotope composition of ostracodes. Palaeogeogr Palaeoclimatol Palaeoecol 176:207–227

Schwalb A (2003) Lacustrine ostracodes as stable isotope recorders of late-glacial and Holocene environmental dynamics and climate. J Paleolimnol 29:267–351

Schwalb A, Dean WE (1998) Stable isotopes and sediments from Pickerel Lake, South Dakota, USA: a 12ky record of environmental changes. J Paleolimnol 20:15–30

Schwalb A, Dean WE (2002) Reconstruction of hydrological changes and response to effective moisture variations from North-Central USA lake sediments. Quat Sci Rev 21:1541–1554

Schwalb A, Locke SM, Dean WE (1995) Ostracode $\delta^{18}O$ and $\delta^{13}C$ evidence of Holocene environmental changes in the sediments of two Minnesota lakes. J Paleolimnol 14: 281–296

Schwalb A, Burns SJ, Kelts K (1999) Holocene environments from stable isotope stratigraphy of ostracods and authigenic carbonate in Chilean Altiplano Lakes. Palaeogeogr Palaeoclimatol Palaeoecol 148:153–168

Schwalb A, Burns SJ, Cusminsky G, Kelts K, Markgraf V (2002) Assemblage diversity and isotopic signals of

modern ostracodes and host waters from Patagonia, Argentina. Palaeogeogr Palaeoclimatol Palaeoecol 187:323–339

Stuiver M (1970) Oxygen and carbon isotope ratios of freshwater carbonates as climatic indicators. J Geophys Res 75:5247–5257

Stuiver M, Reimer PJ, Bard E, Beck JW, Burr GS, Hughen KA, Kromer B, McCormac G, van der Plicht J, Spurk M (1998) INTCAL98 radiocarbon age calibration, 24,000–0 cal BP. Radiocarbon 40:1041–1083

Sun LG, Zhao SP, Liu XD, Xie ZQ, Yin XB, Liu KX, Wu XH (2005) An eco-environmental report on Xisha Archipelago, South China Sea. Chin J Nat 27(2):79–84 (in Chinese with English abstract)

Sun LG, Liu XD, Zhao SP, Liu KX, Wu XH (2007) Sedimentary records: catastrophic marine flooding event occurred on Dongdao Island of South China Sea around 1024 A.D. J Univ Sci Technol China 37(8):986–994 (in Chinese with English abstract)

Trichet J, Fikri A (1997) Organic matter in the genesis of High-island atoll peloidal phosphorites: the lagoonal link. J Sediment Res 67:891–897

Victor R, Fernando CH (1981) Freshwater ostracods (*Crustacea: Ostracoda*) of the subfamily Cyprinotinae Bronstein, 1947 from Malaysia, Indonesia and the Philippines. Hydrobiologia 83:11–27

Vuille M, Werner M, Bradley RS, Keimig F (2005) Stable isotopes in precipitation in the Asian monsoon region. J Geophys Res 110:D23108. doi:10.1029/2005JD006022

Wang JJ (2007) Applications of biomarkers in paleoecology reconstruction in Holocene and characteristics of Antarctic aerosols. Ph.D. Dissertation, University of Science and Technology of China, Hefei, pp 76–94 (in Chinese with English abstract)

Wang JQ (1998) Tropical cyclone distribution of influencing the west oil and gas area of South China Sea. China Offshore Oil Gas (Eng) 10:24–30 (in Chinese)

Wang XL, Wang YM, Ren FM, Li WJ (2006) Interdecadal variations in frequencies of typhoon affecting China during 1951–2004. Adv Clim Change Res 2:135–138 (in Chinese with English abstract)

Webster PJ, Holland GJ, Curry JA, Chang HR (2005) Changes in tropical cyclone number, duration, and intensity in a warming environment. Science 309:1844–1846

Wei GJ, Yu KF, Zhao JX (2004) Sea surface temperature variations recorded on coralline Sr/Ca ratios during Mid-Late Holocene in Leizhou Peninsula. Chin Sci Bull 49:1876–1881

Xia J, Haskell BJ, Engstrom DR, Ito E (1997) Holocene climate reconstructions from tandem trace-element and stable-isotope composition of ostracodes from Coldwater Lake, North Dakota, USA. J Paleolimnol 17:85–100

Yang B, Braeuning A, Johnson KR, Shi YF (2002) General characteristics of temperature variation in China during the last two millennia. Geophys Res Lett 29. doi:10.1029/2001GL014485

Yu KF, Zhao JX, Collerson KD, Shi Q, Chen TG, Wang PX, Liu TS (2004) Storm cycles in the last millennium recorded in Yongshu Reef, southern South China Sea. Palaeogeogr Palaeoclimatol Palaeoecol 210:89–100

Yu KF, Zhao JX, Wei GJ, Cheng XR, Wang PX (2005) Mid-late Holocene monsoon climate retrieved from seasonal Sr/Ca and $\delta^{18}O$ records of *Porites lutea* corals at Leizhou Peninsula, northern coast of South China Sea. Glob Planet Change 47:301–316

Zhang HD (1974) The vegetation of the Xisha Islands. Acta Bot Sin 16(3):183–190 (in Chinese with English abstract)

Zhang XP, Liu JM, Tian LD, He YQ, Yao TD (2004) Variation of $\delta^{18}O$ in precipitation along vapor transport paths. Adv Atmos Sci 21:562–572

Zhu RB, Sun LG, Zhao SP, Xie ZQ, Liu XD, Yin XB (2005) Preliminary studies on methane flux from the ornithogenic soils on Xi-sha atoll, South China Sea. J Environ Sci 17:789–793